

Structure of *Toxoplasma gondii* adenosine kinase in complex with an ATP analog at 1.1 Å resolutionYan Zhang,^a Mahmoud H. el Kouni^b and Steven E. Ealick^{c*}

^aDepartment of Molecular Biology and Genetics, Cornell University, Ithaca, NY 14853, USA, ^bDepartment of Pharmacology and Toxicology, Center for AIDS Research, Comprehensive Cancer Center, University of Alabama at Birmingham, Birmingham, AL 35294, USA, and ^cDepartment of Chemistry and Chemical Biology, Cornell University, Ithaca, NY 14853, USA

Correspondence e-mail: see3@cornell.edu

The obligate intracellular parasite *Toxoplasma gondii* is incapable of synthesizing purine nucleotides *de novo* and relies completely on purines salvaged from the host cells. Adenosine is the preferred precursor and is phosphorylated by adenosine kinase (AK), the most active enzyme in adenosine metabolism in *T. gondii*. AK thus represents a potential chemotherapeutic target for the treatment of *T. gondii* infections. The previously solved structures of unliganded AK and AK in complex with adenosine (or 7-iodotubercidin) and an ATP analog revealed a novel catalytic mechanism. A domain closure triggered by a GG switch upon adenosine binding sequesters the adenosine and γ -phosphate of ATP from the solvent. The formation of the anion hole induced by the ATP binding completes the structural requirements for catalysis. In the current study, the structure of a binary complex of AK and the non-hydrolysable ATP analog AMP-PCP was determined to 1.1 Å resolution. The overall structure is similar to the apoenzyme, with an open conformation. AMP-PCP is bound in two relaxed conformations and without anchoring by Arg136. The induced anion hole is the same as that in the ternary complex AK–adenosine–AMP-PCP. This structure provides direct evidence that ATP binding at millimolar concentrations does not require adenosine binding as a prerequisite.

Received 16 August 2005

Accepted 21 October 2005

PDB Reference: AK–AMP-PCP, 2abs, 2abssf.

1. Introduction

Toxoplasma gondii adenosine kinase (ATP, adenosine 5'-phosphotransferase; EC 2.7.1.20; AK) catalyzes the phosphorylation of adenosine to adenosine monophosphate (AMP) using ATP as the phosphate donor. It is an important enzyme in the purine-nucleoside salvage pathway and the most active enzyme in adenosine metabolism in *T. gondii*, a protozoan parasite (Krug *et al.*, 1989). Like all the intracellular parasites, *T. gondii* lacks a *de novo* purine-biosynthesis pathway and must depend on preformed purines salvaged from the host cells for its purine requirements (el Kouni, 2003; Krug *et al.*, 1989). Adenine, adenosine, hypoxanthine and inosine are required for purine-nucleotide biosynthesis in *T. gondii* because the parasites are able to convert adenine to guanine nucleotides but not the reverse (Krug *et al.*, 1989). Of all the purine precursors, adenosine is the preferred substrate and is incorporated into the nucleotide at a tenfold higher rate than the others. The incorporation of adenosine starts with phosphorylation of AMP by AK. There are no other nucleoside kinase or phosphotransferase activities detected in *T. gondii* (Krug *et al.*, 1989). The critical role and the high activity of AK in adenosine metabolism in *T. gondii* make it an attractive chemotherapeutic target. Intensive studies have been carried out to identify potential compounds as subver-

sive substrates of *T. gondii* AK in order to develop chemotherapeutic agents against this widely spread parasite (el Kouni *et al.*, 1999; Iltzsch *et al.*, 1995; Rais *et al.*, 2005; Yadav *et al.*, 2004).

T. gondii AK is a monomeric protein with 363 residues. Kinetic studies show a K_m of 1.9 μM for adenosine and 54.3 μM for ATP (Darling *et al.*, 1999). The enzyme requires a divalent cation for its activity and is active over the pH range 5.0–9.0 (Recacha *et al.*, 2000). The structures of *T. gondii* AK in the apo form, in complex with adenosine and β,γ -methyleneadenosine 5'-triphosphate (AMP-PCP, a non-hydrolysable ATP analog) and in complex with 7-iodotubercidin and AMP-PCP have been determined (Schumacher *et al.*, 2000). The structures of *T. gondii* AK reveal a novel catalytic mechanism. Upon adenosine binding, a conserved dipeptide Gly68–Gly69 at the active site triggers a rigid-body rotation of 30° of the lid domain, resulting in occlusion of the adenosine and the γ -phosphate of ATP from the solvent. ATP binding induces the formation of an anion hole, which completes the structural requirements for catalysis (Schumacher *et al.*, 2000; Zhang *et al.*, 2004). Based on the sequence and structural homology, *T. gondii* AK is classified as a member of the ribokinase superfamily (Schumacher *et al.*, 2000; Zhang *et al.*, 2004). The structures of more than ten members of this superfamily have been solved, including *Escherichia coli* ribokinase (Sigrell *et al.*, 1998), human adenosine kinase (Mathews *et al.*, 1998), *Bacillus subtilis* 4-methyl-5- β -hydroxy-ethylthiazole kinase (Campobasso *et al.*, 2000), *Thermococcus litoralis* ADP-dependent glucokinase (Ito *et al.*, 2001), *Salmonella typhimurium* 4-amino-5-hydroxymethyl-2-methylpyrimidine phosphate kinase (Cheng *et al.*, 2002), sheep pyridoxal kinase (Li *et al.*, 2002), *Thermus thermophilus* 2-keto-3-deoxygluconate kinase (Ohshima *et al.*, 2004), *B. subtilis* Yxko protein (Zhang *et al.*, 2002) and *Salmonella enterica* aminimidazole riboside kinase (Zhang *et al.*, 2004). The structural characteristic of the enzymes in this superfamily is a central eight-stranded β -sheet that is flanked by eight structurally conserved α -helices, five on one side and three on the other. The active site is located in a shallow cleft along one edge of the β -sheet, with the phosphate-acceptor hydroxyl group and the γ -phosphate of ATP close together in the middle of the groove and the substrate and ATP binding at the ends.

In the current study, the structure of *T. gondii* AK with the bound non-hydrolysable ATP analog AMP-PCP was determined to 1.1 Å resolution. The overall structure is very similar to the apoenzyme, except for the formation of the anion hole. The binary structure suggests that nucleoside binding is not a prerequisite for ATP binding.

2. Experimental procedures

2.1. Protein expression and purification

The AK gene was excised between the *Nde*I and *Sac*I sites from the previously described overexpression plasmid pET21a (Recacha *et al.*, 2000) and spliced into vector pET28a, which encodes a sequence for an N-terminal hexahistidine tag. Both

vectors were sequenced at the Biotechnology Resource Center at Cornell and showed the same errors. One base change leads to a mutation of Gly270 to a serine. There are a few changes (some single-base insertions and deletions) at the 3' end of the gene, which alter the position of the stop codon and change the C-terminus from FTSLPC to FTFTSG; however, the changes in primary sequence do not alter the enzyme activity (data not shown). The new recombinant plasmid was transformed into *E. coli* strain BL21(DE3) (Novagen). A starter culture of the transformed cells was inoculated into 1 l LB containing 50 $\mu g ml^{-1}$ kanamycin. The cells were grown at 310 K until the OD₆₀₀ reached 0.6. Expression was induced by addition of isopropyl β -D-thiogalactopyranoside to a final concentration of 1 mM at 298 K. The cells were harvested after 20 h by centrifugation at 3000g for 20 min at 277 K and were stored at 193 K.

All purification steps were carried out at 277 K. Cells were resuspended in 1/25 of the original cell-culture volume of buffer A (50 mM sodium phosphate, 300 mM sodium chloride pH 8.0) and lysed by two passes through a French press at 172 MPa. The clarified debris-free cell extract was mixed for 1 h with Talon IMAC resin (BD) pre-equilibrated with buffer A. The protein-bound resin was poured into a column and then washed with buffer B (50 mM sodium phosphate, 300 mM sodium chloride, 10 mM imidazole pH 8.0). AK was eluted from the resin with buffer C (50 mM sodium phosphate, 300 mM sodium chloride, 300 mM imidazole pH 8.0) and buffer-exchanged using an Econo-Pac 10DG column (Bio-Rad) into buffer D (20 mM Tris, 10 mM MgCl₂, 5 mM dithiothreitol pH 8.0). The purity of AK was determined by Coomassie-stained SDS-PAGE and found to be greater than 95% (data not shown). The purified protein was then concentrated to 15 mg ml⁻¹ by ultrafiltration using a 30 kDa cutoff concentrator (Amicon) and stored at 193 K. The protein concentrations were determined by the Bradford method (Bradford, 1976) using bovine serum albumin as the standard.

2.2. Crystallization

All crystallization experiments were carried out at 295 K using the hanging-drop vapor-diffusion method. Each drop contained 1 μl protein solution and 1 μl reservoir solution. The protein solution contained 18 mg ml⁻¹ AK, 2 mM AMP-PCP and 0.3 mM 6-[(4-nitrobenzyl)thio]-9- β -D-ribofuranosyl-purine (NBMPR) in buffer D with 8% ethanol. Ethanol was used to dissolve NBMPR as it is not soluble in water. The reservoir solution for the optimized conditions contained 30% PEG 4000, 0.2 M ammonium acetate, 10 mM magnesium chloride, 0.1 M sodium citrate pH 6.1. Crystals appeared within 10 d and attained their maximum size (0.2 \times 0.1 \times 0.1 mm) in about one month. Preliminary X-ray analysis showed that the crystals belong to the orthorhombic space group $P2_12_12_1$. The crystals contain one molecule per asymmetric unit, with a Matthews coefficient of 2.2 Å³ Da⁻¹ and a solvent content of 44.3%.

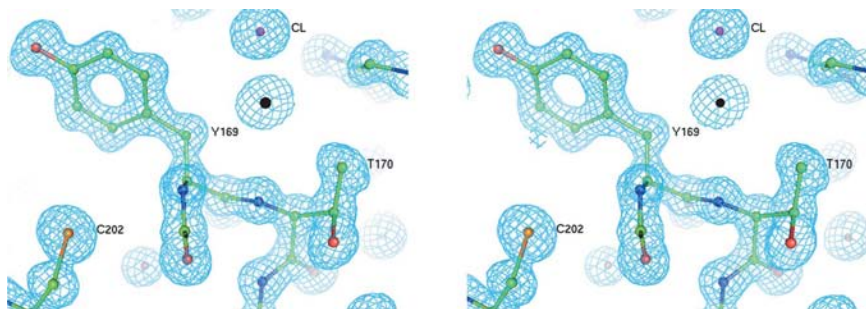


Figure 1
Stereoview of a σ -weighted electron-density map contoured at 1.5σ . The residues are shown in ball-and-stick representation with O atoms in red, C atoms in green and N atoms in blue.

Table 1
Data-collection and refinement statistics.

Values for the outer resolution shell are given in parentheses.

Data collection	
Wavelength (Å)	0.9777
Resolution (Å)	1.1
Space group	$P2_12_12_1$
Unit-cell parameters	
<i>a</i> (Å)	60.05
<i>b</i> (Å)	67.92
<i>c</i> (Å)	83.19
No. of reflections	399904
No. of unique reflections	129879
Redundancy	3.1 (1.9)
Completeness (%)	93.7 (71.9)
R_{sym}^\dagger (%)	6.2 (27.4)
$I/\sigma(I)$	13.6 (2.8)
Refinement	
Total No. of non-H atoms	3417
No. of protein atoms	2896
No. of ligand atoms	64
No. of water O atoms	457
No. of reflections in refinement	122947
No. of reflections in test set	6466
R factor ‡ (%)	14.3
R_{free}^\S (%)	17.3
R.m.s. deviation from ideal geometry	
Bonds (Å)	0.01
Angle distances (Å)	0.03
Ramachandran plot	
Most favored region (%)	94.3
Additionally allowed region (%)	4.4
Generously allowed region (%)	0.7
Disallowed region (%)	0.7

$^\dagger R_{\text{sym}} = \sum_i |I_i - \langle I \rangle| / \sum_i \langle I \rangle$, where $\langle I \rangle$ is the mean intensity of N reflections with intensities I_i and common indices h, k and l . $^\ddagger R$ factor = $\sum_{hkl} ||F_{\text{obs}}| - k|F_{\text{calc}}|| / \sum_{hkl} |F_{\text{obs}}|$, where F_{obs} and F_{calc} are the observed and calculated structure factors, respectively. § For R_{free} , the sum is extended over a subset of reflections (5%) excluded from all stages of refinement.

2.3. X-ray data collection and processing

All data were collected at cryogenic temperatures. For cryoprotection, the crystals were transferred into a mixture of Paratone and paraffin in a volume ratio of 1:2 and then flash-frozen in liquid nitrogen. Data were collected to 1.1 Å resolution at the NE-CAT 8-BM beamline at the Advanced Photon Source using a Quantum-315 CCD detector (Area Detector Systems Corp.). Two passes of data were collected. The high-resolution pass was collected over a range of 205°

using 15 s exposures for each 0.3° oscillation at a crystal-to-detector distance of 180 mm in the unbinned mode. The low-resolution pass was collected over a range of 125° using 5 s exposures for each 0.5° oscillation at a crystal-to-detector distance of 350 mm in the binned mode. The *HKL2000* suite (Otwinowski & Minor, 1997) of programs was used for integration and scaling of all data sets. Details of data collection and processing are given in Table 1.

2.4. Structure determination and refinement

The structure of the complex was determined by molecular replacement using the previously published unliganded AK structure (PDB code 1lio) as the search model. Cross-rotation and translation functions were performed in the *CNS* software package (Brünger *et al.*, 1998) using the data between 10 and 4 Å resolution. A solution was obtained with a correlation coefficient of 0.45. The subsequent refinement was performed using *SHELX* (Sheldrick & Schneider, 1997) followed by manual remodeling with the computer-graphics program *MI-fit* (Molecular Images Software). As the model improved, AMP-PCP was modeled into the density at the ATP-binding site. Bond-distance and bond-angle restraints for AMP-PCP were generated using the program *PRODRG* (Schüttelkopf & van Aalten, 2004). In the late stages of refinement, one chloride ion and one sodium ion were included in the model based on the coordination geometry for each ion, bond distance and refined B factors. The introduction of anisotropic displacement parameters reduced the R factor and R_{free} by 4.0 and 3.3%, respectively. There was still undefined residue density at the active site until the end of the refinement. The R factor and R_{free} are 14.3 and 17.3%, respectively. The final refinement statistics are given in Table 1.

Figures were prepared using *PyMOL* (DeLano, 2002), *MOLSCRIPT* (Kraulis, 1991) and *RASTER3D* (Merritt & Bacon, 1997).

3. Results and discussion

3.1. Overall structure of AK-AMP-PCP

The crystal structure of *T. gondii* AK with the non-hydrolysable ATP analog bound was solved by molecular replacement. The final model, refined at 1.1 Å resolution, contains 2896 protein atoms, one AMP-PCP molecule with two conformations and 457 water molecules. Residues 1–9 and 238–247 are disordered and were not built into the model. The Ramachandran plot shows 99.3% of the residues in the allowed regions and two residues (Arg83 and Ser198) in the disallowed region. Pro12 adopts a *cis* conformation. Both Arg83 and Ser198 are located in non-standard turns and are represented by clear electron density. A representative section of the electron density is shown in Fig. 1.

The complex structure consists of two domains: a large core domain and a small lid domain. The large core domain contains an $\alpha\beta\alpha$ three-layer sandwich. The central β -sheet includes nine strands with a topology of $\beta 6 \uparrow \beta 5 \uparrow \beta 1 \uparrow \beta 9 \uparrow \beta 10 \uparrow \beta 11 \uparrow \beta 12 \uparrow \beta 13 \downarrow \beta 14 \uparrow$. All of the strands

are parallel except for strand 13, which is antiparallel to its neighboring strands. Four α -helices ($\alpha 3$, $\alpha 4$, $\alpha 11$ and $\alpha 12$) flank one side of the β -sheet and six α -helices ($\alpha 5$, $\alpha 6$, $\alpha 7$, $\alpha 8$, $\alpha 9$, and $\alpha 10$) lie on the opposite side. Of these ten α -helices, all except $\alpha 12$ are approximately antiparallel to the strands of the central β -sheet. The small lid domain consists of a twisted five-stranded β -sheet ($\beta 4 \downarrow \beta 2 \uparrow \beta 7 \uparrow \beta 8 \downarrow \beta 3 \downarrow$) that is stabilized by two amphipathic α -helices ($\alpha 1$ and $\alpha 2$).

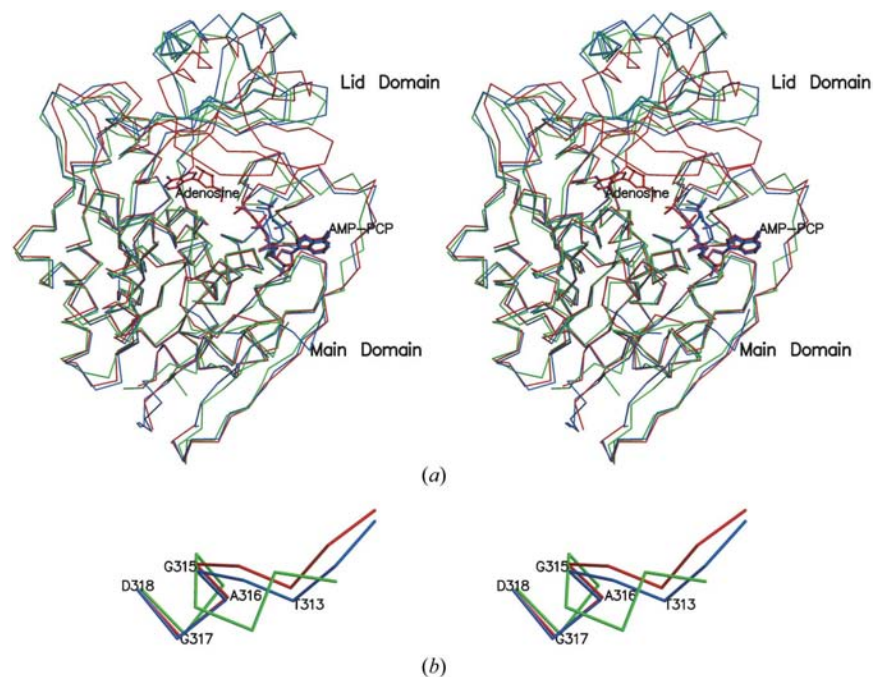


Figure 2

Stereoview of the superposition of apo AK (green), the binary complex AK-AMP-PCP (blue) and the ternary complex AK-adenosine-AMP-PCP (red). (a) Superposition of the C^α traces. The lid domain is at the top, while the main domain is at the bottom. The adenosine and ATP analog are shown in ball-and-stick representation when applicable. (b) Superposition of the anion hole. Gly315, Ala316, Gly317 and Asp318 form the anion hole when AMP-PCP binds and pushes Thr313 away.

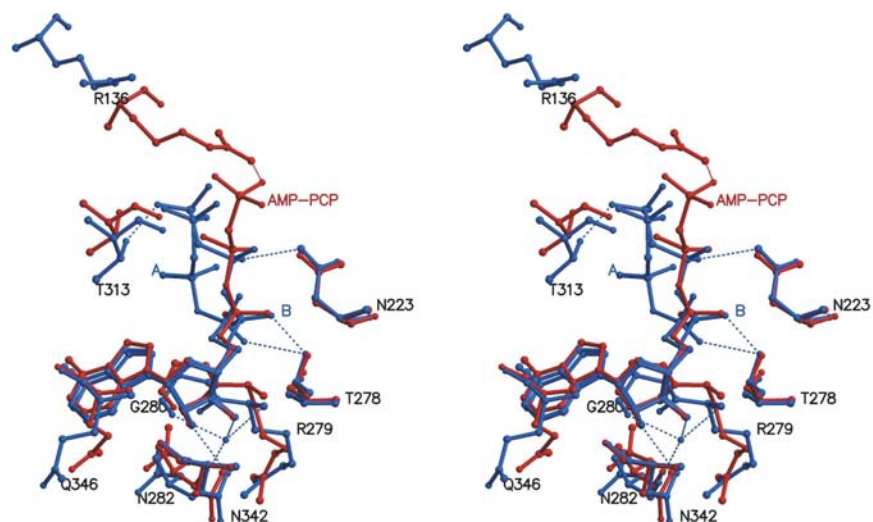


Figure 3

Stereoview of the superposition of the ATP-binding sites of the binary complex AK-AMP-PCP and the ternary complex AK-adenosine-AMP-PCP. The binary complex is shown in blue and the ternary complex in red. The residues and the AMP-PCP are shown in ball-and-stick representations. The two conformations of AMP-PCP in the binary complex are labelled A and B. The residues are labelled by the single-letter amino-acid code and the residue number.

3.2. No global conformational changes are induced by ATP-analog binding

Several structures of *T. gondii* AK in various complexes have been determined previously (Schumacher *et al.*, 2000). These structures reveal that conformational changes induced by substrate binding are required for catalysis. A global conformational change of lid-domain closure is induced by the binding of adenosine (or the subversive substrate 7-iodotubercidin), followed by local conformational changes induced by the binding of ATP. Consistent with those structures, the binary complex of AK and AMP-PCP does not show global conformational changes and the lid domain remains open when the ATP analog is bound. A comparison with the unliganded form of AK (PDB code 1lio) shows a root-mean-square deviation (r.m.s.d.) of 1.4 Å for pairwise comparisons of the C^α atoms of all ordered residues. The major differences between the two structures occur in three loop regions (Fig. 2). The first loop, connecting residue 307 and residue 318, is at the ATP-binding site and includes the residues forming the anion hole. The second loop, connecting residue 233 and residue 252, is disordered in the binary structure of AK and AMP-PCP. The third loop, connecting residue 264 and residue 272, is disordered in the unliganded form of AK. The last two loops are both involved in crystal packing in the cases in which they are ordered.

3.3. Residue electron density at the nucleoside-binding site

The active site of AK is located along one edge of the central β -sheet in the large core domain, with the adenosine-binding site near the lid domain and the ATP-binding site at the other end (Schumacher *et al.*, 2000). In the later stages of the refinement as the model improved, some pieces of residual electron density appeared at the

adenosine-binding site. The strongest density is above the 14 σ contour level in the $F_o - F_c$ map and sandwiched between the phenyl ring of Tyr169 and the side chain of Leu142. In the crystallization setup, NBMPR was added for the purpose of obtaining a complex of AK and the subversive substrate. Consequently, we tried to model NBMPR into the density. When the S atom was positioned in the strongest density, the ribose and the purine base would be oriented in the same way as the adenosine in the ternary complex AK–adenosine–AMP-PCP. However, the density does not fit the molecule and is not connected through the molecule even at a very low contour level in the $F_o - F_c$ map. In addition, the nitro group would clash with Ile188 and Gly189 in the neighboring molecule. Therefore, NBMPR may not bind at the nucleoside-binding site because the crystal packing at the current conditions precludes the large (4-nitrobenzyl)thio group. No solvent molecules or precipitant molecules could be fitted into the residue density. The density remained undefined to the end of refinement but possibly could represent NBMPR at low occupancy and in an unconventional orientation.

3.4. ATP binding

AMP-PCP is bound at the ATP-binding site, which is located in a shallow groove at the C-terminal end of the β -sheet and mostly exposed to the solvent. The adenosine moiety is identified by clear electron density. The sugar ring adopts the common C3'-*endo* conformation and the glycosidic torsion angle is in an *anti* conformation with a value of -167° . The O2' atom of the ribose makes a hydrogen bond to the atom of Asn342 N $^{\delta}$, while the O3' atom forms a hydrogen bond with a water molecule that in turn interacts through hydrogen bonds with the carbonyl O atoms of Gly280 and Asn282 and the amide N atom of Arg279. The purine base does not make any direct interactions with the enzyme. In the ternary complex AK–adenosine–AMP-PCP, the N3 atom accepts a hydrogen bond from Gln346 N $^{\epsilon}$, which has a different conformation (Fig. 3). Interestingly, residue Gln346 in unliganded AK has the same conformation as the binary complex AK–AMP-PCP. The phosphate tail of AMP-PCP, which makes few interactions with the enzyme, is very flexible and is represented by weak density, alternate conformations and high B factors. There are two major conformations: *A* with about 1/3 occupancy and *B* with about 2/3 occupancy (Fig. 3). One α -phosphate O atom in conformation *A* is hydrogen bonded to the hydroxyl group of Thr278, while a different α -phosphate O atom in conformation *B* is hydrogen bonded to the same hydroxyl group. Consequently, the β -phosphate in conformation *B* flips away, with one O atom accepting a hydrogen bond from Asn223 N $^{\delta}$. However, the β -phosphate in conformation *A* does not make any direct interactions with the enzyme, which may contribute to its lower occupancy than conformation *B*. The γ -phosphates of the two conformations superimpose well. One γ -phosphate O atom forms a hydrogen bond with the hydroxyl group of Thr313. No magnesium ion was found near the phosphate groups, although magnesium chloride was added during crystallization.

In the ternary complex AK–adenosine–AMP-PCP, AMP-PCP is in an extended conformation. The γ -phosphate is hydrogen bonded to Arg136 in the small lid domain and oriented toward the 5'-hydroxyl group of adenosine (Fig. 3). An anion hole, right beside the γ -phosphate, is created following the helix-to-coil transition of residues Gly315, Ala316, Gly317 and Asp318. This GAGD sequence is one of the most highly conserved sequence features and the anion hole may be a common structural characteristic of the entire ribokinase superfamily of proteins (Schumacher *et al.*, 2000; Zhang *et al.*, 2004). The anion hole helps to neutralize accumulated negative charge during the phosphate-group transfer. In the binary complex AK–AMP-PCP, Arg136 is distant from the active site owing to the lack of domain closure and AMP-PCP is in a relaxed conformation. The γ -phosphate pushes away Thr313, which occupies the same position in the unliganded enzyme and induces local conformational changes. As a result, Gly315, Ala316, Gly317 and Asp318 form an anion hole. The local conformational changes and the creation of the anion hole in the binary complex are almost identical to those in the ternary complex AK–adenosine–AMP-PCP (Schumacher *et al.*, 2000) (Fig. 2). Apparently, the formation of the anion hole does not require the extended catalytic conformation of ATP. Only after the closure of the lid domain, which is induced by the binding of the nucleoside, is Arg136 translocated into the active site and ATP positioned into the catalytic conformation.

It has been suggested that adenosine binding may be a prerequisite of ATP binding (Schumacher *et al.*, 2000). In contrast to this hypothesis, the binary structure of AK–AMP-PCP is direct evidence that ATP can actually precede the binding of substrates to the enzyme at concentrations typical of a cell; however, under physiological conditions substrate would normally bind before ATP. This suggests that adenosine binding and ATP binding are two independent processes associated with separate conformational changes. In all the available AK structures, no structure with an occupied nucleoside-binding site and an empty ATP binding site exists. When only adenosine is present, it occupies both the ATP and nucleoside binding sites (Schumacher *et al.*, 2000).

4. Conclusions

The structure of *T. gondii* AK complexed with AMP-PCP was determined at 1.1 Å resolution. The crystals were prepared in the presence of a very insoluble substrate analog, but density for the analog was inconclusive. The AK structure shows a conformation in which substrate-induced global conformational changes do not occur, but the local conformational changes associated with nucleotide binding in the AK–adenosine–AMP-PCP complex are present. These observations suggest that the conformational changes associated with adenosine and ATP are independent and binding under physiological conditions can occur in either order.

This work is based upon research conducted at the North-eastern Collaborative Access Team beamline of the Advanced

Photon Source, supported by award RR-15301 from the National Center for Research Resources at the National Institutes of Health. Use of the Advanced Photon Source is supported by the US Department of Energy, Office of Basic Energy Sciences under contract No. W-31-109-ENG-38. We thank Dr Cynthia Kinsland for the preparation of the His-tagged AK overexpression plasmid. We thank Dr Angela V. Toms for assistance with data collection and Leslie Kinsland for assistance with the preparation of this manuscript. This work was also supported by NIH grant AI052838-01.

References

- Bradford, M. M. (1976). *Anal. Biochem.* **72**, 248–254.
- Brünger, A. T., Adams, P. D., Clore, G. M., DeLano, W. L., Gros, P., Grosse-Kunstleve, R. W., Jiang, J.-S., Kuszewski, J., Nilges, M., Pannu, N. S., Read, R. J., Rice, L. M., Simonson, T. & Warren, G. L. (1998). *Acta Cryst. D* **54**, 905–921.
- Campobasso, N., Mathews, I. I., Begley, T. P. & Ealick, S. E. (2000). *Biochemistry*, **39**, 7868–7877.
- Cheng, G., Bennett, E. M., Begley, T. P. & Ealick, S. E. (2002). *Structure*, **10**, 225–235.
- Darling, J. A., Sullivan, W. J. Jr, Carter, D., Ullman, B. & Roos, D. S. (1999). *Mol. Biochem. Parasitol.* **103**, 15–23.
- DeLano, W. L. (2002). *The PyMOL Molecular Graphics System*. DeLano Scientific, San Carlos, CA, USA. <http://www.pymol.org>.
- Iltzsch, M. H., Uber, S. S., Tankersley, K. O. & el Kouni, M. H. (1995). *Biochem. Pharmacol.* **49**, 1501–1512.
- Ito, S., Fushinobu, S., Yoshioka, I., Koga, S., Matsuzawa, H. & Wakagi, T. (2001). *Structure*, **9**, 205–214.
- el Kouni, M. H. (2003). *Pharmacol. Ther.* **99**, 283–309.
- el Kouni, M. H., Guarcello, V., Al Safarjalani, O. N. & Naguib, F. N. (1999). *Antimicrob. Agents Chemother.* **43**, 2437–2443.
- Kraulis, P. J. (1991). *J. Appl. Cryst.* **24**, 946–950.
- Krug, E. C., Marr, J. J. & Berens, R. L. (1989). *J. Biol. Chem.* **264**, 10601–10607.
- Li, M.-H., Kwok, F., Chang, W.-R., Lau, C.-K., Zhang, J.-P., Lo, S. C. L., Jiang, T. & Liang, D.-C. (2002). *J. Biol. Chem.* **277**, 46385–46390.
- Mathews, I. I., Erion, M. D. & Ealick, S. E. (1998). *Biochemistry*, **37**, 15607–15620.
- Merritt, E. A. & Bacon, D. J. (1997). *Methods Enzymol.* **277**, 505–524.
- Ohshima, N., Inagaki, E., Yasuike, K., Takio, K. & Tahirov, T. H. (2004). *J. Mol. Biol.* **340**, 477–489.
- Otwinowski, Z. & Minor, W. (1997). *Methods Enzymol.* **276**, 307–326.
- Rais, R. H., Al Safarjalani, O. N., Yadav, V., Guarcello, V., Kirk, M., Chu, C. K., Naguib, F. N. & el Kouni, M. H. (2005). *Biochem. Pharmacol.* **69**, 1409–1419.
- Recacha, R., Talalaev, A., DeLucas, L. J. & Chattopadhyay, D. (2000). *Acta Cryst. D* **56**, 76–78.
- Schumacher, M. A., Scott, D. M., Mathews, I. I., Ealick, S. E., Roos, D. S., Ullman, B. & Brennan, R. G. (2000). *J. Mol. Biol.* **296**, 549–567.
- Schüttelkopf, A. W. & van Aalten, D. M. F. (2004). *Acta Cryst. D* **60**, 1355–1363.
- Sheldrick, G. M. & Schneider, T. R. (1997). *Methods Enzymol.* **277**, 319–343.
- Sigrell, J. A., Cameron, A. D., Jones, T. A. & Mowbray, S. L. (1998). *Structure*, **6**, 183–193.
- Yadav, V., Chu, C. K., Rais, R. H., Al Safarjalani, O. N., Guarcello, V., Naguib, F. N. M. & el Kouni, M. H. (2004). *J. Med. Chem.* **47**, 1987–1996.
- Zhang, R. G., Grembecka, J., Vinokour, E., Collart, F., Dementieva, I., Minor, W. & Joachimiak, A. (2002). *J. Struct. Biol.* **139**, 161–170.
- Zhang, Y., Dougherty, M., Downs, D. M. & Ealick, S. E. (2004). *Structure*, **12**, 1809–1821.